

## A coordinated ground-based and IMAGE satellite study of quiet-time plasmaspheric density profiles

Zoë C. Dent,<sup>1</sup> I. R. Mann,<sup>1,6</sup> F. W. Menk,<sup>2</sup> J. Goldstein,<sup>3</sup> C. R. Wilford,<sup>4</sup> M. A. Clilverd,<sup>5</sup> and L. G. Ozeke<sup>1,6</sup>

Received 17 January 2003; revised 29 April 2003; accepted 12 May 2003; published 17 June 2003.

[1] Cold plasma mass density profiles in the plasmasphere have been determined for the geomagnetically quiet day of 19th August 2000 using the cross-phase technique applied to ground-based magnetometer data from the SAMNET, IMAGE and BGS magnetometer arrays. Cross-phase derived mass densities have been compared to electron densities derived from both ground-based VLF receiver measurements, and the IMAGE satellite RPI. The cross-phase results are in excellent agreement with both the VLF and IMAGE observational results, thus validating the cross-phase technique during quiet times. This is the first such coordinated multi-instrument study, and has enabled very few heavy ions to be inferred in the plasmasphere for  $L > 3.45$  on this day. The observational results were compared to plasma mass densities from the SUPIM model and were found to be in excellent agreement. IMAGE EUV data also verified the existence of azimuthal structure in the outer quiet-time plasmasphere.

**INDEX TERMS:** 2768 Magnetospheric Physics: Plasmasphere; 2794 Magnetospheric Physics: Instruments and techniques; 2772 Magnetospheric Physics: Plasma waves and instabilities; 2752 Magnetospheric Physics: MHD waves and instabilities. **Citation:** Dent, Z. C., I. R. Mann, F. W. Menk, J. Goldstein, C. R. Wilford, M. A. Clilverd, and L. G. Ozeke, A coordinated ground-based and IMAGE satellite study of quiet-time plasmaspheric density profiles, *Geophys. Res. Lett.*, 30(12), 1600, doi:10.1029/2003GL016946, 2003.

### 1. Introduction

[2] Since the discovery of the plasmopause by *Carpenter* [1963] and *Gringauz* [1963] the dynamic plasmasphere - plasmopause - plasmatrough system has been extensively monitored using both ground-based and satellite techniques. The dynamics of mass loss and injection processes are not fully understood, in fact the Imager for Magnetopause-to-Aurora Global Exploration (IMAGE) mission is dedicated to better understanding these issues. However, the average position of the plasmopause can be described by empirical models, for example *Orr and Webb* [1975] and *Carpenter and Anderson* [1992]. The majority of these previous studies have investigated electron number

density, and so the behaviour of the ion populations are less well understood.

[3] This letter presents the first coordinated IMAGE satellite and multi-instrument ground-based study of the plasmasphere. Observational results from ground-based magnetometers, VLF receivers, the IMAGE RPI (Radio Plasma Imager) and EUV (Extreme Ultraviolet Imager), and plasma mass densities calculated along flux tubes by SUPIM (Sheffield University Plasmasphere Ionosphere Model) [e.g., *Bailey and Sellek*, 1990] are compared. In a similar plasmatrough study *Loto'aniu et al.* [1999] compared ground-based magnetometer derived plasma mass densities to in-situ electron densities measured by the CRRES satellite.

[4] By assuming a hydrogen plasma, electron number densities (e.g., from the VLF measurements or IMAGE RPI instrument) can be directly converted to plasma mass densities. When these are compared to mass density estimates including heavy ions (e.g., those derived from ground-based magnetometer data or the SUPIM model) this allows inferences to be made about the presence of heavy ions.

[5] Individual techniques cannot provide plasma densities at all local times or L-shells. Currently, the best single-instrument view of the plasmasphere comes from the EUV imager on the IMAGE satellite [*Sandel et al.*, 2000]. This routinely produces remote-sensing images of the helium portion of the plasmasphere, with spatial and temporal resolutions of  $0.1 R_E$  and  $\sim 10$  minutes respectively, in 2-D line-of-sight integrated pictures. Therefore, coordinated multi-instrument observations of a particular plasma population, recorded at different L-shells and/or local times, can offer a unique view of plasma dynamics currently unavailable using a single instrument alone.

### 2. Method and Results

[6] We present observations from 19th August 2000, a geomagnetically quiet day with  $K_p < 2$  during which the magnetosphere was recovering from a  $K_p = 8^-$  storm which occurred seven days previously.

[7] The cross-phase technique compares amplitude and phase spectra, in the ULF range, from latitudinally separated ground-based magnetometer pairs to produce an estimate of the local field line resonant frequency of the field-line whose footprint lies approximately mid-way between the two stations [e.g., *Waters et al.*, 1996; *Menk et al.*, 1999]. As this frequency depends upon the field line length, the ambient magnetic field strength, and the plasma density along the field line, it can be used to obtain an estimate of the equatorial plane plasma mass density [e.g., *Menk et al.*, 1999]. This was achieved by numerically solving the standing toroidal Alfvén wave equation in dipole coordinates, derived by *Radoksi* [1967]; and assuming a radial density distribution  $\sim r^{-3}$ .

<sup>1</sup>Department of Physics, University of York, Heslington, York, UK.

<sup>2</sup>School of Mathematical and Physical Sciences and CRC for Satellite Systems, The University of Newcastle, Newcastle, NSW, Australia.

<sup>3</sup>Department of Physics and Astronomy, Rice University, Texas, USA.

<sup>4</sup>Space and Atmosphere Research Group, Department of Applied Mathematics, University of Sheffield, Sheffield, UK.

<sup>5</sup>British Antarctic Survey, Cambridge, UK.

<sup>6</sup>Now at Dept. of Physics, University of Alberta, Canada.

[8] Data from eight selected stations of the combined SAMNET (U.K. Sub-Auroral Magnetometer Network) and BGS (British Geological Survey) magnetometer array and four stations of the IMAGE (International Monitor for Auroral Geomagnetic Effects) array in northern Europe have been used to produce ten plasma density estimates between  $L = 2.66$  and  $L = 5.85$  from 0625–0750 UT (approximately 0704–0858 LT). One of the magnetometer stations (Thurso,  $58.36^\circ\text{N}$ ,  $3.69^\circ\text{W}$ ,  $L = 3.30$ ) was temporarily deployed as part of the SAMNET array between 18–21st August 2000. The location of these stations are shown as solid squares in Figure 1. Figure 2 shows the cross-phase derived mass densities for this interval. Associated error-bars plotted in Figure 2 relate to uncertainty in identifying field line resonant frequencies using the cross-phase technique, and are typically  $\sim 25\text{--}30\%$ . Other less significant uncertainties are due to assumptions of a toroidal mode wave and the  $r^{-3}$  density dependence assumed in calculating the mass density for the observed resonant frequency. These have not been included in the cross-phase error-bars shown in Figure 2.

[9] The RPI instrument on board the elliptically orbiting IMAGE satellite is able to passively measure the ambient electric field in order to determine the local plasma frequency, and thus the in-situ electron density [e.g., *Reinisch et al.*, 2000; *Goldstein et al.*, 2003]. Data from two orbits are presented. The first pass (orbit 1 in Figure 2), between 0615–0812 UT ( $\sim 0300$  MLT), spanned L-shells between 8.10 and 2.45 and latitudes between  $34^\circ\text{N}$  and  $19^\circ\text{S}$ . The second pass (orbit 2 in Figure 2) was from 1928–2214 UT ( $\sim 0300$  MLT) and spanned L-shells between 3.20 and 7.97 and latitudes between  $24^\circ\text{N}$  and  $25^\circ\text{S}$ . The northern hemisphere geomagnetic field ground footprints of the IMAGE satellite during these two intervals are plotted in Figure 1 using the Tsyganenko 89 magnetic field model (from SSCWeb at <http://www.sscweb.gsfc.nasa.gov>).

[10] Recent observations have suggested that field-aligned density profiles at high altitudes may be almost constant [Goldstein et al., 2001]. Hence the  $\times$  and  $+$  symbols in Figure 2 represent the expected equatorial electron density if the local field-aligned density variation is constant. However, previous studies have also suggested steeper plasma density variations along the field line. Warner and Orr [1979] stated

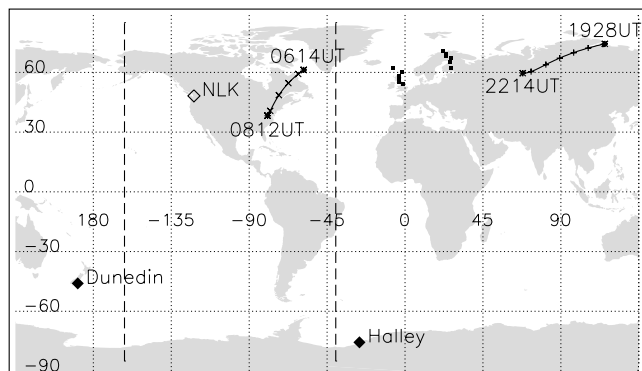


**Figure 1.** Map showing relative geographic positions of the instruments used for this study. IMAGE satellite northern-hemisphere magnetic field traces between 0614–0812 UT and 1928–2214 UT are also shown, with tick marks placed at hh:00 and hh:30 UT.

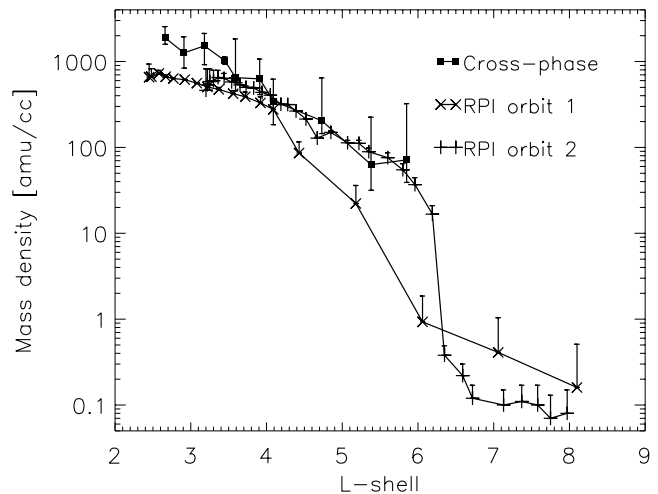


**Figure 2.** Cross-phase and IMAGE RPI derived plasma mass densities with associated error bars (see text for details).

that a plasma density variation of  $r^{-3}$  is appropriate for the plasmasphere. Poulter et al. [1984] calculated that varying the assumed density variation between  $r^{-3}$  and  $r^{-5}$  would alter the deduced density by less than  $\pm 9\%$ . The size of the error bars in Figure 2 shows the difference between the equatorial plane electron number densities if constant and  $r^{-3}$  mapping of RPI densities to the equatorial plane are assumed. The implicit error associated with identifying the in-situ IMAGE RPI electron densities relates to the uncertainty in manually determining the electron plasma frequencies. This error is assumed to be 12% on average; however, this error is not indicated explicitly in Figure 2.

[11] VLF (Very Low Frequency) signals received at two locations have also been used to calculate equatorial plane electron number densities (filled diamond symbols in Figure 1). Doppler whistler-mode signals from the NLK transmitter ( $48.2^\circ\text{N}$ ,  $121.9^\circ\text{W}$ ; open diamond in Figure 1) were received at Dunedin, New Zealand ( $46^\circ\text{S}$ ,  $171^\circ\text{E}$ ) and typically propagate along ducts situated between  $L = 2.0\text{--}2.5$  at the geographic longitude  $\sim 162^\circ\text{W}$  (first dashed line in Figure 1). The delay times used to calculate the equatorial plane electron density were measured at 1000 UT (0000 LT), see Clilverd et al. [1991] for more details. Also, natural lightning-generated whistlers were received at Halley ( $76^\circ\text{S}$ ,  $26^\circ\text{W}$ ) between 0400–0730 UT (0100–0430 LT). These are assumed to be generated in the east-coast region of the USA, and propagate at an assumed longitude of  $\sim 40^\circ\text{W}$  (second dashed line in Figure 1). Eight equatorial plane electron densities in the region of  $L = 4$  were calculated using the Park diffusive equilibrium model no. 1 [Park, 1982] from the Ho and Bernard [1973] 3-point whistler scaling method. The error associated with the VLF-derived electron densities is assumed to be 10% [Ho and Bernard, 1973].

[12] Mass densities have also been calculated using the SUPIM model. SUPIM is an ab-initio model which assumes a dipolar geomagnetic field and solves time dependent equations of continuity, momentum and energy balance to produce estimates of  $\text{O}^+$ ,  $\text{H}^+$ ,  $\text{He}^+$  and  $\text{e}^-$  density along a closed plasmaspheric flux tube as a function of local time for a particular day. Actual values of  $A_p$  and  $f_{10.7}$  are used as inputs for the model. The individual ion densities in the equatorial plane were summed to provide an overall plasma

mass density for 21 L-shells between  $L = 2.57$  and  $L = 6.02$  at 0700 LT.

[13] Figure 3 shows a summary of the plasma density profiles derived using all three observational techniques and from SUPIM (error bars have been omitted for clarity).

### 3. Discussion

[14] In Figure 3 the first IMAGE orbit profile shows a gradual decrease in density with L-shell from  $L \sim 2.45$  to  $L \sim 4$ , beyond which density decreases more rapidly, by over two orders of magnitude across  $2 R_E$ , before again decreasing with L at a gradual rate to  $L = 8.10$ . The second IMAGE orbit profile shows an extended plasmasphere to  $L \sim 6$  where a sharp decrease of density indicates a typical plasmapause. Beyond  $L \sim 6$  in the plasmatrough the density continues to decrease gradually with increasing L-shell. These profiles can be compared to Figure 1 of *Carpenter and Anderson* [1992]. The IMAGE orbit 1 profile is similar to refilling profiles whereas the IMAGE orbit 2 profile is similar to a recently depleted plasmasphere profile, albeit at a very high L-shell. The presence of these two profiles on the same day suggests that azimuthal structure is present in the density distribution in the quiet-time outer plasmasphere.

[15] The Kp-driven empirical model for local-time dependent plasmapause position given by *Orr and Webb* [1975] locates the plasmapause at  $L = 5.44 \pm 0.4$  at 0800 LT (= UT) on this day; in fairly good agreement with the observed results in Figure 3. The predicted plasmapause position appropriate to the RPI density profile for IMAGE orbit 1 is  $0.1 R_E$  inward of this. Hence the differences between the ground-based cross-phase profile (0600–0800 LT) and the first IMAGE pass (0300 LT) cannot be explained by LT differences in model plasmapause location but are indicative of an azimuthally localised density depletion in the outer plasmasphere which is local to IMAGE during orbit 1.

[16] The cross-phase derived plasma mass density profile shows a gradual decrease with L-shell at typical plasmaspheric densities ( $\sim 1000$  amu/cc), and is in agreement with the plasmaspheric part of the IMAGE orbit 2 profile. The VLF derived plasma densities also show a typical plasma-

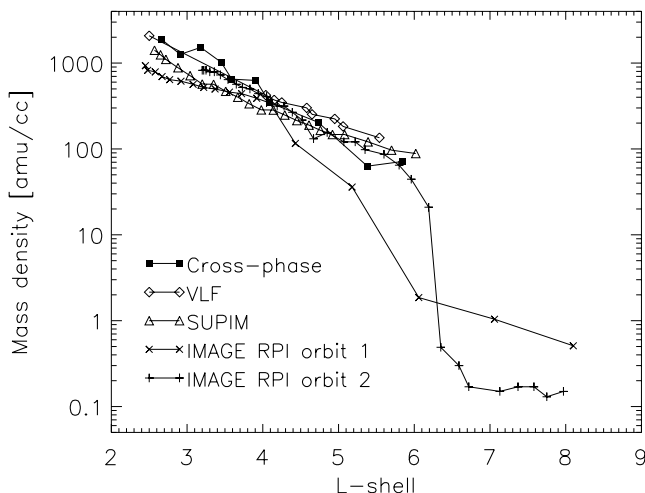


**Figure 3.** Plasma mass density profiles determined using four different techniques.

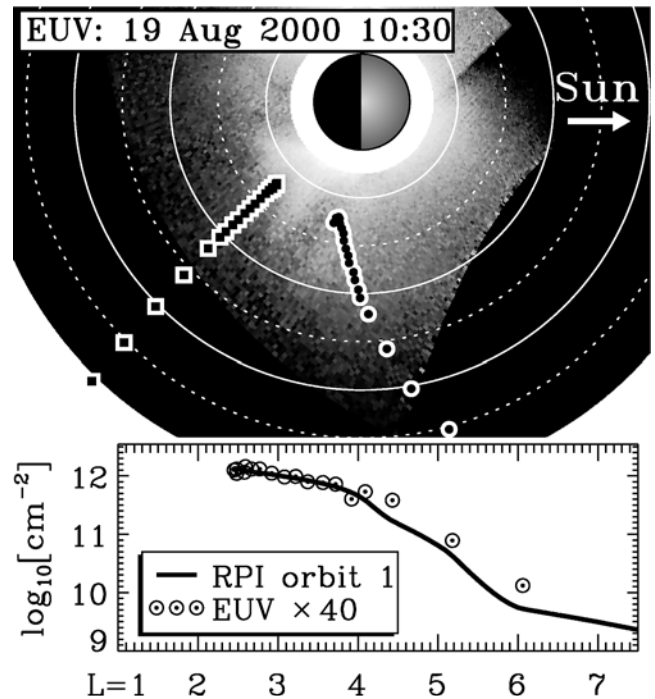


**Figure 4.** IMAGE EUV equatorial intensity at 1030 UT (top panel; see text for details). IMAGE EUV and RPI column abundances along co-rotated orbit 1 (circles and solid line, respectively) for 1030 UT (bottom panel; see text for details).

sphere profile, in good agreement with those profiles derived from the cross-phase technique and from the RPI instrument during IMAGE orbit 2.

[17] The plasmaspheric plasma density profile calculated by the SUPIM model, shown in Figure 3, agrees well with those derived from the three observational techniques, thus validating all of these techniques during a quiet interval. However, local time variation offered by SUPIM (not shown) does not explain the different plasma density profile observed during IMAGE orbit 1.

[18] Figure 4 (top panel) shows the IMAGE EUV equatorial intensity of 30.4 nm ultraviolet light. In this plot, each pixel of the 1030 UT raw EUV image has been mapped to the magnetic equatorial plane assuming a dipole field, as described for single points in *Goldstein et al.* [2003]. The sun is to the right, in the direction of the white arrow; and radial distance in the equatorial plane is shown by the concentric circles, each separated by  $1 R_E$ . Significant azimuthal structure is apparent, particularly in the nightside, consistent with differing RPI density profiles between orbits 1 and 2; this structure being observed to co-rotate in subsequent EUV images (not shown). Squares show the location of the in-situ RPI measurements for orbit 1, and circles show the locations of these plasma elements in the 1030 UT EUV image, assuming co-rotation. The bottom panel shows  $\text{He}^+$  column abundance (circles), calculated from EUV pixel intensity and the observed solar flux at 30.4 nm. Also plotted is the electron column abundance, (solid line) calculated from the observed RPI orbit 1 density data as shown in Figure 3, assuming constant density along magnetic field lines. Aside from the scale factor of 40 there is excellent agreement between the RPI and EUV column density profiles, veri-

fying the existence of an extended outer plasmaspheric density depletion local to RPI orbit 1. The agreement between the ground-based density profiles and RPI orbit 2 (Figure 3) suggests a more azimuthally uniform plasmasphere might be present later following a more extended period of refilling. The EUV intensity versus L profile for 1030 UT and 0730 LT (not shown), appropriate to the VLF measurements in Figure 3, suggest that higher densities may persist to at least  $L = 4.8$  (the edge of the EUV field of view for this LT). This is consistent with ground measurements of a more extended plasmasphere at later local times.

[19] To examine the presence of heavy ions in the plasmasphere we have compared the IMAGE orbit 1 RPI and cross-phase derived plasma densities observed at similar L-shells (within  $0.2 R_E$ ). Assuming all heavy ions are of one species, the inferred number density is 35–64%  $\text{He}^+$  or 7–13%  $\text{O}^+$  for  $L < 3.45$ . Beyond  $L = 3.45$  the observed densities from the two techniques agree within the limit of the errors, suggesting relatively few heavy ions in the outer plasmasphere. This general trend agrees with that of Craven *et al.* [1997], who observed a decrease in  $\text{He}^+$  to  $\text{H}^+$  ratio with increasing radial distance in the plasmasphere. The percent number density of  $\text{He}^+$  calculated by SUPIM increases from 2.9% at  $L = 2.57$  to 6.5% at  $L = 6.02$ , whilst the percent number density of  $\text{O}^+$  is negligible. This may explain the slightly lower SUPIM profile as compared with the cross-phase derived profile at low L-shells in Figure 3.

#### 4. Conclusions

[20] A multi-instrument study of quiet-time magnetospheric cold plasma densities has been presented. Using data collected on 19th August 2000 by the IMAGE RPI instrument, ground-based VLF receivers and ground-based magnetometers, equatorial plane plasma mass density profiles in the plasmasphere have been derived. These profiles were compared to each other and also to that calculated by the SUPIM model. Excellent agreement was obtained, validating the cross-phase technique for monitoring plasmaspheric density profiles during quiet times. Comparison of plasma density profiles suggested that few heavy ions were present beyond  $L = 3.45$ .

[21] Beyond  $L \sim 4$  the two profiles presented for the two IMAGE satellite passes on 19th August 2000 disagree, suggesting azimuthal structure in the outer plasmasphere. IMAGE EUV images verify the gradual plasmopause observed by RPI during orbit 1; quiet-time plasmaspheric azimuthal structure seen in the EUV images being consistent with the in-situ RPI observations differing from orbit to orbit, and with the observations of Moldwin *et al.* [1995] and Carpenter and Lemaire [1997]. Our study illustrates the benefits of using multiple instruments as a means to identify smaller-scale plasma density structures. In the future, multi-instrument studies can be used to monitor geomagnetic storm-time plasmaspheric depletion and refilling processes, and to examine the role of heavy ions during these times.

[22] **Acknowledgments.** The authors thank the institutes who maintain the IMAGE magnetometer array, British Geological Survey, and the SAMNET team for magnetometer data (SAMNET is a PPARC National Facility operated by the University of York); Neil Thompson for providing Dunedin VLF receiver data; Bill Sandel for the calculations of electron and

$\text{He}^+$  column abundance; Bodo Reinisch for providing IMAGE RPI data; and Lord Thurso of Caithness for providing the field-site for the Thurso magnetometer. Z.C.D. and C.R.W. were supported by PPARC studentships and L.G.O. was supported by PPARC grant PPA/G/O/2001/2001/00021. F.W.M. thanks the Australian Research Council for financial support. Work at Rice was supported by NASA contract NASS-96020 as part of the IMAGE mission. The IMAGE EUV investigation at the University of Arizona (Bill R. Sandel, PI) is funded under NASA contract NASS-96020 with Southwest Research Institute.

#### References

- Bailey, G. J., and R. Sellek, A mathematical model of the Earth's plasmasphere and its application in a study of  $\text{He}^+$  at  $L = 3$ , *Ann. Geophys.*, **8**, 171–190, 1990.
- Carpenter, D. L., Whistler evidence of a “knee” in the magnetospheric ionization density profile, *J. Geophys. Res.*, **68**, 1675–1682, 1963.
- Carpenter, D. L., and R. R. Anderson, An ISEE/whistler model of equatorial electron density in the magnetosphere, *J. Geophys. Res.*, **97**, 1097–1108, 1992.
- Carpenter, D. L., and J. Lemaire, Erosion and recovery of the plasmasphere in the plasmopause region, *Space Sci. Rev.*, **80**, 153–179, 1997.
- Clilverd, M. A., A. J. Smith, and N. R. Thomson, The annual variation in quiet time plasmaspheric electron density, determined from whistler mode group delays, *Planet. Space Sci.*, **39**, 1059–1067, 1991.
- Craven, P. D., D. L. Gallagher, and R. H. Comfort, Relative concentration of  $\text{He}^+$  in the inner magnetosphere as observed by the DE 1 retarding ion mass spectrometer, *J. Geophys. Res.*, **102**, 2279–2289, 1997.
- Goldstein, J., et al., Latitudinal density dependence of magnetic field lines inferred from Polar plasma wave data, *J. Geophys. Res.*, **106**, 615–621, 2001.
- Goldstein, J., et al., Identifying the plasmopause in IMAGE EUV data using IMAGE RPI in situ steep density gradients, *J. Geophys. Res.*, **108**, 1147, doi:10.1029/2002JA009475, 2003.
- Gringauz, K. I., The structure of the ionized gas envelope of the earth from direct measurements in the USSR of local charged particle concentrations, *Planet. Space Sci.*, **11**, 281–296, 1963.
- Ho, D., and L. C. Bernard, A fast method to determine the nose frequency and minimum group delay of a whistler when the causative spheric is unknown, *J. Atmos. Terr. Phys.*, **35**, 881–887, 1973.
- Loto'aniu, T. M., et al., Plasma mass density in the plasmatrough: Comparison using ULF waves and CRRES, *Geophys. Res. Lett.*, **26**, 3277–3280, 1999.
- Menk, F. W., et al., Monitoring spatial and temporal variations in the day-side plasmasphere using geomagnetic field line resonances, *J. Geophys. Res.*, **104**, 19,955–19,969, 1999.
- Moldwin, M. B., et al., The fine-scale structure of the outer plasmasphere, *J. Geophys. Res.*, **100**, 8021–8029, 1995.
- Orr, D., and D. C. Webb, Statistical studies of geomagnetic pulsations with periods between 10 and 70 sec and their relationship to the plasmopause region, *Planet. Space Sci.*, **23**, 1169–1178, 1975.
- Park, C. G., Whistlers, in *CRC Handbook of Atmospheric*, edited by H. Volland, CRC Press, Boca Raton, Florida, USA, 1982.
- Poulter, E. M., et al., Plasmatrough ion mass densities determined from ULF pulsation eigenperiods, *Planet. Space Sci.*, **32**, 1069–1078, 1984.
- Radoski, H. R., A note on oscillating field lines, *J. Geophys. Res.*, **72**, 418–419, 1967.
- Reinisch, B. W., et al., The Radio Plasma Imager investigation on the IMAGE spacecraft, *Space Sci. Rev.*, **91**, 319–359, 2000.
- Sandel, B. R., et al., The extreme ultraviolet imager investigation for the IMAGE mission, *Space Sci. Rev.*, **91**, 197–242, 2000.
- Warner, M. R., and D. Orr, Time of flight calculations for high latitude geomagnetic pulsations, *Planet. Space Sci.*, **27**, 679–689, 1979.
- Waters, C. L., J. C. Samson, and E. F. Donovan, Variation of plasmatrough density derived from magnetospheric field line resonances, *J. Geophys. Res.*, **101**, 24,737–24,745, 1996.
- Z. C. Dent, I. R. Mann, and L. G. Ozeke, Department of Physics, University of York, Heslington, York, YO10 5DD, UK. (zdent@space.ualberta.ca; imann@space.ualberta.ca; lozeke@phys.ualberta.ca)
- F. W. Menk, School of Mathematical and Physical Sciences and CRC for Satellite Systems, The University of Newcastle, Callaghan, NSW, Australia. (Fred.Menk@newcastle.edu.au)
- J. Goldstein, Department of Physics and Astronomy, Rice University, Texas, USA. (jerru@rice.edu)
- C. R. Wilford, Space and Atmosphere Research Group, Department of Applied Mathematics, University of Sheffield, Sheffield, UK. (C.Wilford@sheffield.ac.uk)
- M. A. Clilverd, British Antarctic Survey, Cambridge, UK. (m.clilverd@bas.ac.uk)